Noninnocent Role of Na^+ Ions in the Binding of the *N*-Phenyl-2-naphthylammonium Cation as a Ditopic Guest with Cucurbit[7]uril

Suma S. Thomas, Hao Tang, & Cornelia Bohne

May 2019

Noninnocent Role of Na^+ Ions in the Binding of the *N*-Phenyl-2-naphthylammonium Cation as a Ditopic Guest with Cucurbit[7]uril

Suma S. Thomas, Hao Tang,[†] and Cornelia Bohne*

Department of Chemistry and Centre for Advanced Materials and Related Technologies (CAMTEC), University of Victoria, PO Box 1700 STN CSC, Victoria, BC V8W 2Y2, Canada

ABSTRACT: Na^+ ions influence the mechanism for the binding of the ditopic guest *N*-phenyl-2-naphthylammonium cation (Ph-AH^+-Np) to cucurbit[7]uril (CB[7]) by facilitating, at increased Na^+ concentrations, the formation of a higher order complex. Binding of the larger naphthyl moiety of Ph-AH^+-Np forms the Ph-AH^+-Np@CB[7] 1:1 complex (where "@" represents an inclusion complex) at low Na^+ ion concentrations (≤5 mM), whereas the inclusion of the smaller phenyl moiety in CB[7] (CB[7]@Ph-AH^+-Np) is transient. Ph-AH^+-Np@CB[7] is formed by reactions with free CB[7] and CB[7]•Na^+ (where "•" represents an exclusion complex) with displacement of the Na^+ cation. Because of the latter reaction, the dissociation of Ph-AH^+-Np@CB[7] is faster at higher Na^+ concentrations. At high Na^+ concentrations (≥25 mM), the Na^+ ion stabilizes the inclusion of the phenyl moiety in CB[7] by capping the portal of CB[7]. The dynamics of the capped Na^+•CB[7]@Ph-AH^+-Np 1:1 complex is slower than in the absence of Na^+ capping. This stabilization of the phenyl moiety inclusion in CB[7] by Na^+ leads to the formation of the Na^+•CB[7]@Ph-AH^+-Np@CB[7] 2:1 host–guest complex, where each moiety of the ditopic guest is included in a different CB[7]. The opposing roles of Na^+ cations in the formation of the two 1:1 complexes are essential for the switch in mechanism with changes in Na^+ concentration and provide an example of systems chemistry, where new properties arise in the form of an increased diversity of complexes and altered complexation dynamics that depend on the system's composition.

INTRODUCTION

Complexity arises when a sufficient number of interacting components lead to the emergence of properties that cannot be predicted from the behavior of the system's individual components. Such behavior constitutes the basis of systems chemistry.[1–5] From the perspective of supramolecular chemistry, host–guest complexes are frequently described as supermolecules, with a focus on one complex and not the entire system. This approach is valid for isolable host–guest complexes. However, for systems that are in equilibrium or in which multiple complexes are present, focusing on the main complex may miss a wealth of information contained within the system. In this context, we explored the mechanistic complexity for the binding of a ditopic guest, *N*-phenyl-2-naphthylamine (Ph-A-Np), which has moieties of different sizes, to cucurbit[7]uril (CB[7], Scheme 1) in the presence of Na^+, which bind competitively to the portals of CB[7].

Cucurbit[*n*]urils (CB[*n*]s) are macrocyclic hosts that bind cationic hydrophobic guests with high affinity.[6–9] CB[*n*]s have found applications in functional nanostructures,[10,11] catalysis,[6,12–14] stimuli-responsive gels,[15–18] enzymatic assays,[19–21] and drug delivery,[22–25] and also as self-sorting systems.[26–29] In addition, CB[*n*]s bind metal cations, hydronium ions, or ammonium ions at their carbonyl-lined portals.[30–32] The structure of the guest determines the binding mechanism with CB[*n*]s.[33–46] A small guest, such as the 2-naphthyl-1-ethylammonium cation (NpH^+, Scheme 1), slips in and out of the CB[7] cavity,[43] whereas the larger 2-aminoanthracenium cation (AH^+, Scheme 1) forms a competitive exclusion complex that slows the formation dynamics of the inclusion complex.[45] Guests that require distortion of CB[7] to form a complex, such as berberine, show slower association and dissociation dynamics,[44] despite having equilibrium constants with CB[7] similar to that observed for NpH^+.[43]

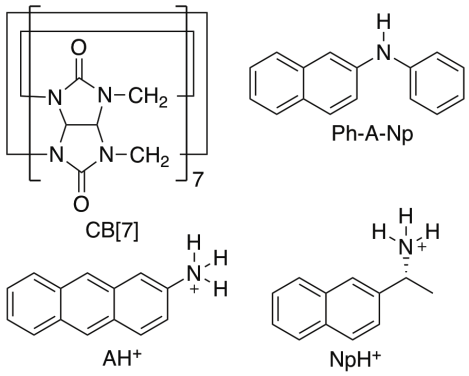

Scheme 1. Structures of cucurbit[7]uril, *N*-phenyl-2-naphthylamine, 2-aminoanthracenium cation, and *R*-(+)-2-naphthyl-1-ethylammonium cation.

A different approach for exploring the mechanistic diversity for guest binding to CB[7] is to focus on the competitive binding of metal cations. The binding of metal cations to the portals of CB[*n*] affects the mass balance for the host by decreasing the availability of free CB[*n*] for guest binding.[43,47–51] As metal

cations do not interact with the host–guest complex in this case, they are considered to have a passive role, with the presence of a cation leading to a decrease in the guest's overall binding constant with CB[*n*]. An exception to this behavior has been observed for small guests, where the CB[6]–guest complex stability is increased when metal cations act as a lid to the complex.[52–54] Cations binding to the CB[7] portals have also been reported to play a role in the formation of extended assemblies with a guest.[55]

In this study, we report that Na^+ has an active role in modifying the binding behavior of Ph-AH^+-Np with CB[7]. Ph-AH^+-Np was chosen as a ditopic guest because the naphthyl moiety has an optimal size to fit within CB[7], whereas the smaller phenyl moiety does not. Our expectations were that the dynamics for phenyl inclusion would be faster than that for naphthyl inclusion and that phenyl inclusion in CB[7] would be transient. This expectation was met at low Na^+ ion concentrations. However, at high Na^+ ion concentrations, the inclusion dynamics of the phenyl moiety was slowed by the capping of CB[7] with a Na^+ ion, leading to the formation of a 2:1 host–guest complex (Na^+•CB[7]@Ph-AH^+-Np@CB[7], where the symbols "•" and "@" represent exclusion and inclusion complexes, respectively). This switch in mechanism is a consequence of the presence of different binding motifs with CB[7]: the optimally sized naphthyl moiety of Ph-A-Np, the suboptimal phenyl moiety of Ph-A-Np, and Na^+ as a competitor for guest binding. Two of these binding motifs, namely, the phenyl moiety and Na^+ ion, are involved in a synergistic interaction, as the individual binding of each of these moieties with CB[7] is weak. Increasing the system complexity by using a ditopic guest uncovered the active role that Na^+ ions can play in the formation and dynamics of higher order complexes with CB[*n*]s, showing that metal cations present in the system cannot be assumed to be innocent bystanders that just modulate the mass balance for free CB[*n*]. The current work shows, through kinetic studies, that the effect of Na^+ on the host-guest dynamics is non-linear in the sense that the effect of cations cannot be extrapolated from studies at one concentration or a limited concentration range of the metal cation. This finding has an impact on the design of functional supramolecular systems containing CB[n]s, where the function is directly related to the dynamics of the system.

RESULTS AND DISCUSSION

Positively charged guests bind more strongly with CB[*n*]s than neutral ones.[6,8] This difference dictates the choice of experimental conditions where the protonation state of the guest has to be taken into consideration. The stronger binding of cationic species to CB[*n*]s leads to a higher pK_a for the complexed guest when compared with the pK_a of the guest in water.[56–60] In this study, we used changes in fluorescence intensities to determine binding isotherms and kinetics. These measurements require the guest's fluorescence to change when bound to CB[7]. The binding of Ph-A-Np to CB[7] was studied at pH 1.8 so that Ph-A-Np was deprotonated and neutral when free in aqueous solution but protonated and positively charged when bound to CB[7] (see the Supporting Information for the determination of the pK_a values, Figure S1), ensuring a larger change in fluorescence intensity upon binding of Ph-A-Np to CB[7]. At pH 1.8, the pseudo-first-order rate constant for the protonation of neutral Ph-A-Np bound to CB[7] was estimated to have a lifetime of 40 ns by assuming the same protonation rate constant as previously measured for the AH^+@CB[7] complex (1.5×10^9 M^{-1} s^{-1}).[45] Therefore, the protonation of Ph-A-Np included in CB[7] is much faster than the binding kinetics measured using stopped-flow experiments (>1 ms). In this case, to analyze our kinetic data, we can assume that Ph-A-Np is neutral in water and "instantaneously" protonated (Ph-AH^+-Np) when complexed.

The changes in the Ph-A-Np fluorescence intensities upon addition of CB[7] were qualitatively different at low and high Na^+ ion concentrations. At low Na^+ ion concentrations, a continuous decrease in the fluorescence intensity was observed as the CB[7] concentration was raised, whereas at high Na^+ ion concentrations, the initial decrease was followed by an intensity increase. This difference in behavior indicated the presence of different host–guest complexes in solutions with different Na^+ ion concentrations. Fluorescence lifetime measurements were used to identify these different species. In the absence of CB[7] at pH 5.1, which is well above the pK_a of Ph-A-Np (pK_a < 1), the fluorescence decay for Ph-A-Np in water was monoexponential with a lifetime of 4.8 ns. This lifetime was assigned to the excited state decay of neutral Ph-A-Np. At pH 0.7, close to the pK_a of Ph-A-Np, the fluorescence decay yielded two lifetimes. The longer lifetime of 1.7 ns was assigned to the neutral guest. This lifetime is shorter than the one measured at pH 5.1 because aromatic amines undergo fluorescence quenching by protons under acidic conditions.[61,62] The estimated rate constant (k_q) for the excited state Ph-A-Np quenching by protons (Figure S2) is between the k_q values reported for neutral α- and β-naphthyl amines.[62] The second shorter lifetime of less than 0.5 ns was assigned to the emission from protonated Ph-AH^+-Np. These results are consistent with the fluorescence intensity of Ph-A-Np in water being higher than that of the protonated guest in the CB[7] complex.

At pH 1.8, the fluorescence decay of Ph-A-Np in water was monoexponential and yielded a lifetime of 4.6 ns, confirming that only neutral Ph-A-Np was present at this pH. In the presence of CB[7] and Na^+ ions, three lifetimes of 1.1, 4.6 and 11 ns were obtained from the fluorescence emission decay (for details, see the Supporting Information). The 4.6 ns lifetime corresponds to the emission of Ph-A-Np in water, whereas the 1.1 and 11 ns lifetimes correspond to CB[7] complexes (Scheme 2). The shorter 1.1 ns lifetime is assigned to the emission from Ph-AH^+-Np bound to CB[7] with the naphthyl group included in the CB[7] cavity, where in the absence of CB[7], this lifetime for excited Ph-AH^+-Np is less than 0.5 ns. The observation of a shorter lifetime for the excited guest in the complex (1.1 ns) than for the neutral guest in water (4.6 ns) is consistent with the decrease in fluorescence intensity observed with the addition of low concentrations of CB[7], irrespective of the Na^+ ion concentration. The longer lifetime of 11 ns is assigned to a higher order complex of Ph-AH^+-Np with two CB[7]s, where the naphthyl and phenyl moieties are bound to two different CB[7] molecules (Scheme 2). These assignments are supported by the binding isotherm studies and kinetics measurements described below. The nonradiative deactivation of the singlet excited state of Ph-A-Np is likely to include a mode coupled to the rotation of either the naphthyl group or the phenyl ring, as

has been observed for other fluorophores that contain a naphthalene and phenyl groups bound to an amine.[63] Therefore, the increase in intensity and lengthening of the singlet excited state lifetime are consistent with the location of the naphthyl and phenyl moieties in different CB[7]s to form a 2:1 complex.

Scheme 2. Species identified in time-resolved fluorescence experiments at pH 1.8. In water, the guest is deprotonated (Ph-A-Np), and in the CB[7] complexes, the guest is protonated (denoted by the blue dot) with a shorter excited state lifetime for the 1:1 complex and a longer lifetime for the 2:1 complex.

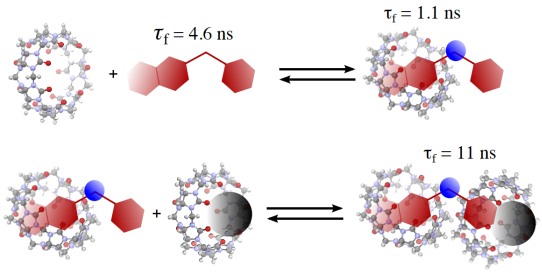

The pre-exponential factors associated with each lifetime in the fluorescence decays provide a measure of the contribution of each emissive species to the decay (Tables S1 and S2). The three lifetimes were present at all Na^+ concentrations, indicating that the higher order complex is always formed. For Na^+ ion concentrations of 5 mM or lower, the contribution of the higher order complex is less than 10%, and the formation of the higher order Na^+•CB[7]@Ph-AH^+-Np@CB[7] complex was not included in the analysis of the binding isotherms and kinetics. The effect of the formation of the higher order complex was studied for Na^+ ion concentrations of 25 mM or higher, where the contribution of this complex is higher.

The results for the two Na^+ ion concentration regimes are described separately because the host–guest binding mechanism depends on the Na^+ ion concentration. The fluorescence emission spectra for Ph-A-Np in the presence of CB[7] and 2 or 4 mM Na^+, defined as the low Na^+ concentration regime, showed a continuous decrease in intensity accompanied by a blue shift of the emission peak. Binding isotherms constructed from the fluorescence data fit well to a 1:1 binding model (Figure 1 and Figure S3). These adequate fits show that the presence of a small amount of the higher order complex does not significantly affect the fit of the binding isotherm, as the intensity change for the higher order complex is positive and a significant contribution from this species would lead to nonrandom residuals for the fit of the binding isotherm to a 1:1 binding model. The overall equilibrium binding constants (eq 1, where $[CB[7]]_{GF}$ = [CB[7]] + [CB[7]•Na^+] + [Na^+•CB[7]•Na^+]) for the formation of the Ph-AH^+-Np@CB[7] 1:1 complex obtained from the fits of the binding isotherms were $(3.6 \pm 0.1) \times 10^5$ and $(2.6 \pm 0.1) \times 10^5$ M^{-1} at 2 and 4 mM Na^+, respectively. The decrease observed at the higher Na^+ ion concentration is due to the higher concentration of Na^+•CB[7]•Na^+, which is not involved in the formation of the host–guest complex.

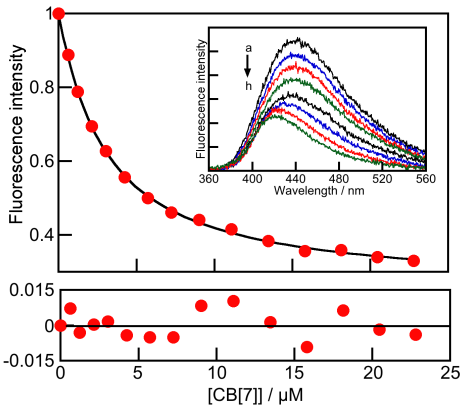

Figure 1. Fit of the binding isotherm to a 1:1 binding model and the corresponding residuals for the binding of 0.5 μM Ph-A-Np with CB[7] in the presence of 2 mM Na^+. The inset shows the fluorescence emission spectra of 0.5 μM Ph-A-Np in the absence (a) and presence (b–h) of up to 23 μM CB[7].

$$\beta_{01} = \frac{[\text{Ph-AH}^+\text{-Np@CB[7]}]}{[\text{CB[7]}]_{GF}\,[\text{Ph-A-Np}]} \qquad (1)$$

The kinetics for the mixing of Ph-A-Np with CB[7] in the presence of 2, 4, and 5 mM Na^+ had two relaxation processes and leveled off within 0.1 s (Figure 2). The amplitude of the final change in fluorescence from the kinetic experiment matched the intensity changes observed in the binding isotherm experiments (Figure S4). This result confirms that the kinetics was measured for a sufficiently long period of time for the system to reach equilibrium and that all kinetic processes were captured in the stopped-flow traces.

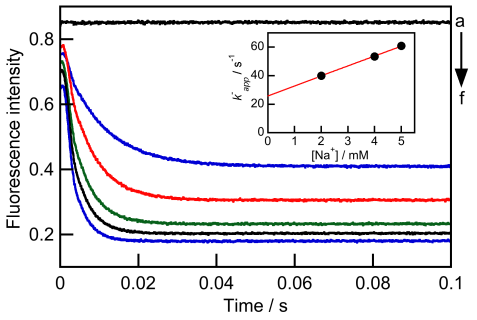

Figure 2. Stopped-flow traces for the mixing of 0.5 μM Ph-A-Np with 0 (a, black), 5 (b, blue), 10 (c, red), 15 (d, green), 20 (e, black), and 25 μM (f, blue) CB[7] in the presence of 2 mM Na^+. The inset shows the dependence of the dissociation rate constant on the Na^+ ion concentration for Ph-AH^+-Np binding with CB[7].

The time scale for the slow relaxation process is of the same order of magnitude as the kinetics for NpH^+ binding to CB[7],[43] and this process was assigned to the binding of the naphthyl moiety of Ph-A-Np to CB[7]. The presence of a fast component indicates that a second relaxation process occurs, which has kinetics close to the time resolution of the stopped-flow experiments (~1 ms). The rate constant for the fast component was fixed to 1000 s^{-1} for the purpose of fitting the overall kinetics. This fast kinetics is consistent with the transient binding of the

phenyl moiety of Ph-A-Np to CB[7] because the phenyl ring is too small to fill the CB[7] cavity optimally.

The observed rate constants for the formation of the Ph-AH$^+$-Np@CB[7] 1:1 complex (k_{obs1}) obtained from the analysis of the slow relaxation process are related to the apparent association (k_{app}^+) and dissociation (k_{app}^-) rate constants (eq 2). The observed rate constants increased linearly with the total CB[7] concentration (Figure S5). Analysis of the data at different Na$^+$ ion concentrations showed that both k_{app}^+ and k_{app}^- changed with the concentration of Na$^+$. The decrease in the value of k_{app}^+ at higher Na$^+$ ion concentrations is consistent with the binding of Na$^+$ to CB[7]•Na$^+$ to form Na$^+$•CB[7]•Na$^+$, leading to a decrease in the concentration of host available to bind the guest. The k_{app}^- value increased linearly with the Na$^+$ ion concentration (inset, Figure 2), indicating that the dissociation of Ph-AH$^+$-Np@CB[7] is accelerated by Na$^+$. This result is consistent with the complexation of the guest with CB[7]•Na$^+$ (eq 6 in Scheme 3), where association of Ph-A-Np displaces Na$^+$ but the guest is also displaced by the metal cation in the reverse reaction.

$$k_{\text{obs1}} = k_{\text{app}}^+[\text{CB[7]}] + k_{app}^- \quad (2)$$

Scheme 3. Mechanism for the binding of Ph-AH$^+$-Np with CB[7] at low Na$^+$ ion concentrations.[a]

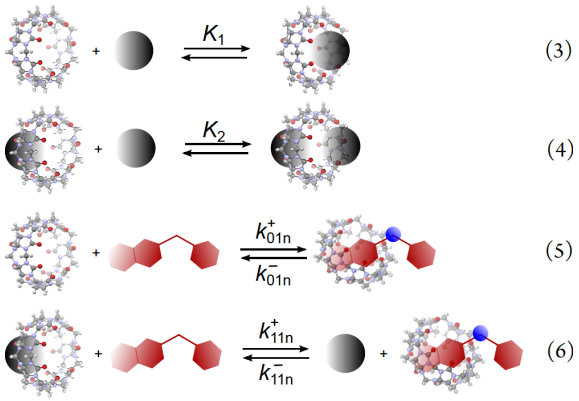

[a], The first subscript indicates the number of Na$^+$ cations bound to CB[7] and the second subscript indicates the number of guest molecules bound to CB[7]. Any "zeros" not followed by an integer are not shown. The subscripts "n" and "p" (see below) denote the inclusion of the naphthyl and phenyl moieties, respectively. At pH 1.8, the guest is not protonated in water but is protonated in the CB[7] complex, as denoted by the blue dot.

The overall equilibrium constant for the 1:1 complex (β_{01}) is equal to the ratio of the apparent association and dissociation rate constants. The β_{01} values calculated from these rate constants were $(3.0 \pm 0.3) \times 10^5$ M^{-1} at 2 mM Na$^+$ and $(2.1 \pm 0.1) \times 10^5$ M^{-1} at 4 mM Na$^+$. These values are close to but somewhat lower than the values determined from the binding isotherms ($(3.6 \pm 0.1) \times 10^5$ and $(2.6 \pm 0.1) \times 10^5$ M^{-1}). In the analysis used for the kinetics, we assumed that the concentrations of free CB[7] and CB[7]•Na$^+$ were not significantly altered by the transient formation of the complex in which the phenyl moiety is included. The fact that a lower β_{01} value was obtained from the kinetic experiment suggests that this assumption is not completely valid. The formation of the transient phenyl inclusion complex can be viewed in the same manner as the transient formation of an exclusion complex, as observed for AH$^+$.[45] The transient formation of the CB[7]@Ph-AH$^+$-Np complex lowers the concentration of host available for the formation of the Ph-AH$^+$-Np@CB[7] complex, which affects the bimolecular reaction involving the host, as reflected by a decrease in the association rate constant. In contrast, the value of the dissociation rate constant is not affected by the presence of the transient complex, as the dissociation process is either unimolecular or depends on the Na$^+$ concentration (eqs 5 and 6 in Scheme 3 and eq 7). This decrease in the association rate constant without a change in the dissociation rate constant leads to the smaller β_{01} value. Determination of the equilibrium constant for the formation of the phenyl inclusion complex (CB[7]@Ph-AH$^+$-Np) from the kinetic data was not possible because the expected curvature for the dependence of the observed rate constant on the CB[7] concentration[45] was not observed, suggesting a low value for this equilibrium constant.

The apparent dissociation rate constant (k_{app}^-) is related to the two reactions for formation of Ph-AH$^+$-Np@CB[7] (eqs 5 and 6 in Scheme 3) by:

$$k_{\text{app}}^- = k_{01\text{n}}^- + k_{11\text{n}}^-[\text{Na}^+] \quad (7)$$

The values obtained for k_{11n}^- and k_{01n}^- from the fit of the dependence of k_{app}^- on the Na$^+$ ion concentration were $(6.9 \pm 0.2) \times 10^3$ M^{-1} s^{-1} and 26 ± 1 s^{-1}, respectively. A slight decrease in the apparent association rate constant (k_{app}^+) from $(1.16 \pm 0.02) \times 10^7$ to $(1.08 \pm 0.02) \times 10^7$ M^{-1} s^{-1} was observed when the Na$^+$ ion concentration was raised from 2 to 5 mM. A decrease in k_{app}^+ is expected owing to the formation of the Na$^+$•CB[7]•Na$^+$ complex, which reduces the concentration of CB[7] species that bind the guest, namely, free CB[7] and CB[7]•Na$^+$. Unlike the variation in k_{app}^- with the Na$^+$ ion concentration, the changes in the k_{app}^+ values are too small for the precise determination of individual values for k_{11n}^+ and k_{01n}^+, and studies at higher Na$^+$ ion concentrations, as required to observe a further decrease in k_{app}^+, were precluded by the switch in mechanism discussed below.

The unimolecular dissociation rate constant (k_{01n}^-) for Ph-AH$^+$-Np@CB[7] of 26 s^{-1} is lower than the dissociation rate constant for the corresponding complex of CB[7] with NpH$^+$ (55 s^{-1})[43] but higher than that for the corresponding complex with AH$^+$ (10 s^{-1}),[45] suggesting that the position of the positive charge with respect to the hydrophobic moiety of the guest has an influence on the residence time of the guest in the CB[7] complex. Steric hindrance from the additional phenyl ring in Ph-AH$^+$-Np probably plays no role or a minor one, as a dissociation rate constant of 50 s^{-1} was observed for the dissociation of a flavylium cation, where the two aromatic rings are in closer proximity to the positive charge located on the 1-benzopyrylium moiety.[46]

The binding of Ph-AH$^+$-Np to CB[7]•Na$^+$ differed from the behavior observed for NpH$^+$, which only binds to free CB[7], as indicated by the dissociation rate constants for NpH$^+$, which did not change when the Na$^+$ ion concentration was raised from 50 to 200 mM.[43] In this high Na$^+$ ion concentration range, the dissociation rate constant for Ph-AH$^+$-Np from CB[7], which includes the bimolecular reaction with Na$^+$, would have been 370–1400 s^{-1}, and the dynamics of the complex would have

been too fast to measure in stopped-flow experiments. Our current results do not provide full insights into the reasons for the difference in the binding abilities of Ph-AH$^+$-Np and NpH$^+$ with CB[7]•Na$^+$. One possible explanation is that the position of the positive charge with respect to the aromatic ring affects the ability of the guest to expel the Na$^+$ bound to the opposite portal of CB[7], which would occur for Ph-AH$^+$-Np but not NpH$^+$. A second possibility is that the binding of the neutral guest, Ph-A-Np, would lead to a deeper inclusion into the CB[7] cavity expelling the Na$^+$ before protonation of the guest in the complex occurs. Evidence supporting the latter suggestion is the slow down by one order of magnitude, when compared to the rate constant in water, of the protonation rate constant to form AH$^+$@CB[7][45], while for a CB[7] guest where the protonation site is exposed to water the protonation rate constant is the same as in water.[64]

The increase in the Na$^+$ ion concentration changes the relative concentrations of CB[7] and CB[7]•Na$^+$. Although Ph-A-Np binding to CB[7] and CB[7]•Na$^+$ is competitive at low Na$^+$ ion concentrations because the concentration of CB[7] is higher or similar to that of CB[7]•Na$^+$ ([CB[7]]/[CB[7]•Na$^+$] = 4.0, 1.9, and 1.5 for [Na$^+$] = 2, 4, and 5 mM, respectively, Table S3), at high Na$^+$ ion concentrations, the predominant host species is CB[7]•Na$^+$ ([CB[7]]/[CB[7]•Na$^+$] = 0.31, 0.18, and 0.16 for [Na$^+$] = 25, 40, and 50 mM, respectively) and the binding of the guest to free CB[7] is minimized. At Na$^+$ ion concentrations of 25 mM Na$^+$ or higher, the addition of CB[7] led to an initial decrease in the guest fluorescence intensity, followed by an intensity increase (Figure 3 and Figure S6). The magnitude of the decrease is much smaller than that observed at low Na$^+$ ion concentrations (Figure 1) and the CB[7] concentration that defines the intensity minimum in the binding isotherm occurs at lower CB[7] concentrations as the Na$^+$ concentration is raised (7–9 mM for 50 mM Na$^+$, Figure 3 and 18–20 mM for 25 mM Na$^+$, Figure S6). The decrease in the fluorescence intensity is due to the formation of the 1:1 complex (see above). The formation of this complex occurs initially with the addition of CB[7] followed by the formation of a different complex, in which the fluorescence intensity of Ph-AH$^+$-Np increases. This intensity increase can be explained by both aromatic rings of the guest being in constrained environments that preclude their rotation (Scheme 4). The involvement of Na$^+$ cations in the formation of the higher order complex was assigned based on the absence of this intensity increase at low Na$^+$ ion concentrations and the dependence of the position of the minimum intensity in the binding isotherms with respect to the CB[7] concentration on the Na$^+$ ion concentration (inset, Figure 3). These binding isotherms could not be fitted because a constant intensity value was not achieved by the highest CB[7] concentration used and because the 1:1 complexes between the naphthyl or phenyl groups and CB[7] did not exhibit different spectroscopic signatures.

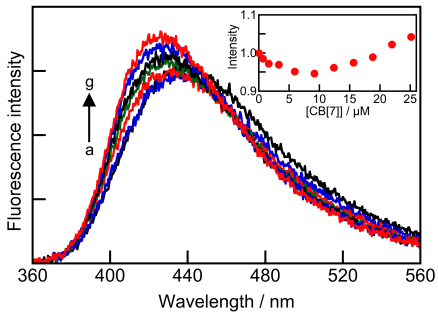

Figure 3. Fluorescence emission spectra of 0.5 μM Ph-A-Np in the absence (a) and presence (b–g) of up to 25 μM CB[7] at a Na$^+$ ion concentration of 50 mM. The inset shows the dependence of the fluorescence intensity on the total CB[7] concentration, as determined from emission spectra normalized to the spectrum in the absence of CB[7].

Scheme 4. Mechanism for the binding of Ph-AH$^+$-Np with CB[7] at high Na$^+$ ion concentrations.

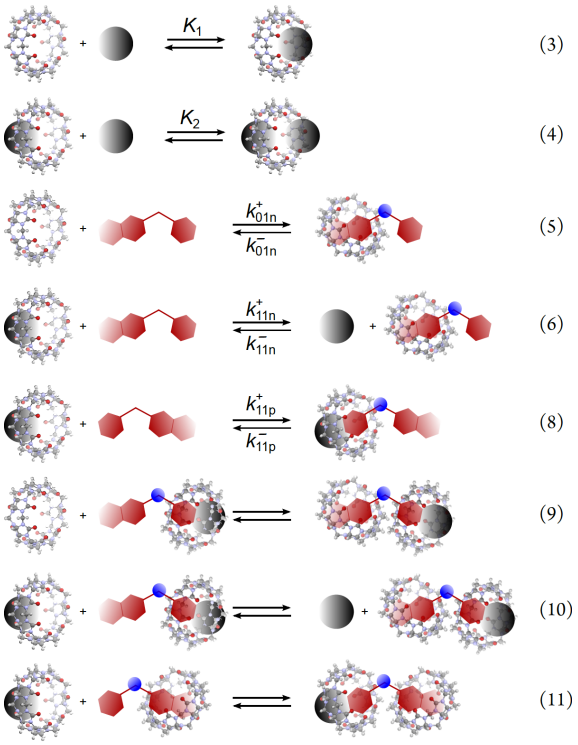

The initial fast kinetics at low Na$^+$ ion concentrations slowed down at high Na$^+$ ion concentrations (inset, Figure 4 and Figures S7 and S8). The absence of an offset for the kinetics at high Na$^+$ ion concentrations indicates that the binding dynamics of the phenyl group with CB[7] became slower, as a faster process would appear as an increased initial offset. This slowdown is assigned to the formation of the 1:1 complex where phenyl is included in a CB[7] that is capped by Na$^+$ (Na$^+$•CB[7]@Ph-AH$^+$-Np). The Na$^+$ capped complex is more stable than the transient binding of the phenyl moiety to CB[7] observed at low Na$^+$ ion concentrations for the uncapped complex.

The initial decay in intensity was followed by a growth that did not level off within 0.2 s. The amplitude of the growth increased when the Na^+ ion concentration was raised (Figure 4 and Figure S8). This kinetic behavior agrees with the binding isotherm studies, where the initial intensity decrease at low CB[7] concentrations is due to the formation of 1:1 complexes, whereas the subsequent intensity increase is due to the formation of the higher order Na^+•CB[7]@Ph-AH^+-Np@CB[7] complex.

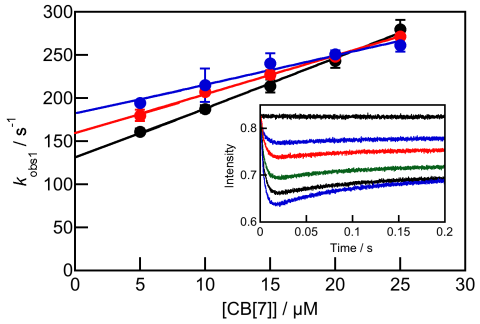

Figure 4. Dependence of the observed rate constant for the decay on the CB[7] concentration when Ph-A-Np was mixed with CB[7] at Na^+ ion concentrations of 25 (black), 40 (red), and 50 mM (blue). The error bars correspond to average deviations from 2 independent experiments. When no error bar is visible, the errors are smaller than the height of the data point. The inset shows the kinetics for the mixing of 0.5 μM Ph-A-Np with 0 (top, black), 5 (blue), 10 (red), 15 (green), 20 (black), and 25 μM (bottom, blue) CB[7] in the presence of 50 mM Na^+.

The kinetics was adequately fit to two relaxation processes, one corresponding to the decay and the other to the growth kinetics. The values of the observed rate constants for the growth kinetics could not be obtained with precision because the kinetics did not level off, which also led to a mismatch of the amplitudes from the stopped-flow and binding isotherm studies. This result suggests that the formation of the higher order complex is not fully captured on the time scale of the kinetic experiment. The kinetics was also measured at very high CB[7] concentrations (160–340 μM) in the presence of 25 and 50 mM Na^+, when the formation of the 1:1 complexes is faster than the 1 ms time resolution of the experiment. In this case, the formation of the two 1:1 complexes can be treated as a fast pre-equilibrium that appears as an initial offset and only the growth kinetics is observed (Figure S9). This growth leveled off within 3 and 1 s at 25 and 50 mM Na^+, respectively, showing that the rate for this reaction increases when the Na^+ concentration is raised. Analysis of this kinetics required the inclusion of three relaxation processes, suggesting that the formation of the higher order complex could occur through different pathways (eqs 9–11 in Scheme 4). However, this kinetics was not further analyzed because at these very high CB[7] concentrations, some of the observed processes could be due to CB[7] complexation to Na^+ cations without the inclusion of guests, which may lead to the formation of aggregates, as has been observed in the gas phase.[65] The determination of how the formation of such CB[*n*]–cation complexes influences the kinetics of the Ph-A-Np and CB[7] system is beyond the scope of the current work.

The decay kinetics at high Na^+ ion concentrations was adequately fit to one relaxation process, suggesting that the rates for the formation of the Ph-AH^+-Np@CB[7] and Na^+•CB[7]@Ph-AH^+-Np 1:1 complexes are similar and cannot be differentiated. The observed rate constant for the decay depends linearly on the CB[7] concentration (Figure 4). The apparent association and dissociation rate constants (eq 2) correspond to the combined formation of the two 1:1 complexes (eqs 5, 6, and 8 in Scheme 4). Both these rate constants vary with the Na^+ ion concentration. The decrease in the slope for the dependence of k_{obs1} on the CB[7] concentration (Figure 4) is attributed to the formation of the Na^+•CB[7]•Na^+ complex, to which the guest cannot bind. The increase for k_{app}^- (Figure 5) is due to the contribution of the binding of the naphthyl moiety of the guest to CB[7]•Na^+, as observed for the k_{obs1} dependence at low Na^+ concentrations (eq 7 and inset, Figure 2).

The dependence of the apparent dissociation rate constant on the Na^+ ion concentration at high Na^+ concentrations is linear, but the dependence has a lower slope and a higher intercept when compared with the extrapolated values for the dependence observed at low Na^+ ion concentrations (Figure 5), underscoring the switch in mechanism when the Na^+ ion concentration is changed (Scheme 5). If the same mechanism operated in both Na^+ ion concentration regimes, the slopes should be the same because the dissociation of Ph-AH^+-Np@CB[7] in the reaction with Na^+ ions occurs under pseudo-first-order conditions as the concentration of Na^+ (mM) is much higher than the concentration of CB[7] (<50 μM).

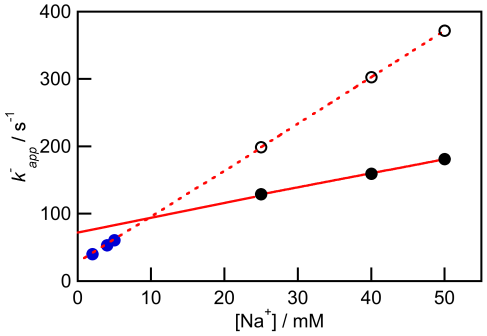

Figure 5. Dependence of the apparent dissociation rate constant (solid circles) on the Na^+ concentration for Ph-A-Np binding with CB[7] at high Na^+ concentrations. The black open circles show the predicted dependence for the binding of Ph-A-Np to CB[7] if the mechanism that occurs at low Na^+ concentrations is assumed (dotted line). The blue solid circles are the experimental k_{app}^- values at low Na^+ ion concentrations.

Scheme 5. Mechanistic representation of the effect of Na^+ ion concentration on the distribution of species for the Ph-A-Np/CB[7] system.

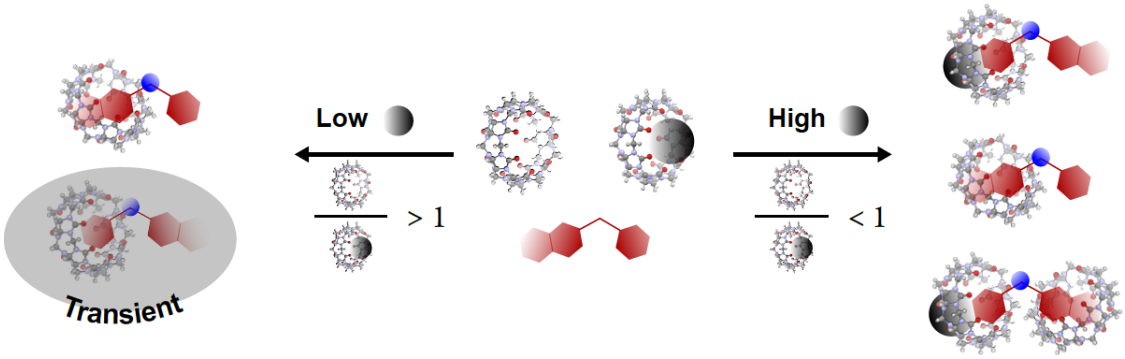

As a first approximation, the intercept for the dependence of k_{app}^{-} on the Na^+ concentration (Figure 5) corresponds to the unimolecular dissociation rate constant of the guest from both 1:1 complexes (eqs 5 and 8) and can be equated to the sum of the corresponding dissociation rate constants ($k_{01n}^{-} + k_{01p}^{-}$). From the intercept, we calculated the dissociation rate constant of the phenyl inclusion complex (Na^+•CB[7]@Ph-AH^+-Np) as 51 ± 2 s^{-1}, which is of the same order of magnitude as the unimolecular dissociation rate constant for the naphthyl moiety for Ph-AH^+-Np@CB[7] (26 s^{-1}). This similarity is consistent with the observation of only one relaxation process for the decay kinetics at high Na^+ ion concentrations.

The switch in mechanism with different Na^+ ion concentrations occurs because of the opposing roles that Na^+ plays in the competitive pathways for the formation of the two CB[7] 1:1 complexes with the ditopic guest. The competitive binding of the naphthyl and phenyl moieties of Ph-A-Np to free CB[7] followed our expectations based on the size complementarity between these moieties and the CB[7] cavity. Phenyl inclusion in free CB[7] is fast and transient because this moiety is too small to fill the cavity of the host optimally. Therefore, the binding of the phenyl group is less favored thermodynamically than the binding of the naphthyl moiety to free CB[7]. In the absence of an active role for Na^+, we might have observed the binding of a second CB[7] to the Ph-AH^+-Np@CB[7] complex at very high CB[7] concentrations (>100 µM), as has been observed for the binding of a flavylium cation.[46] However, the active role for Na^+ introduced competitive pathways, which led to a Na^+ concentration-dependent switch in mechanism (Scheme 5).

Na^+ ions sped up the dissociation of the guest from the Ph-AH^+-Np@CB[7] complex through a bimolecular reaction to form CB[7]•Na^+, whereas Na^+ slowed down the dissociation of the phenyl moiety through the formation of the capped Na^+•CB[7]@Ph-AH^+-Np complex. One possible explanation for this slowdown is that the Na^+ ion bound to one of the portals impedes the ready access of water molecules to fill the CB[7] cavity as the guest leaves through the opposite portal, slowing the exit of the guest and leading the Na^+•CB[7]@Ph-AH^+-Np 1:1 complex to have higher stability than CB[7]@Ph-AH^+-Np. The molecularities for the dissociation reactions of these two complexes are different. Displacement of the guest from Ph-AH^+-Np@CB[7] by Na^+ is a bimolecular reaction, whereas dissociation of the guest from the phenyl inclusion complex Na^+•CB[7]@Ph-AH^+-Np is unimolecular because at high Na^+ concentrations, the association of Na^+ with CB[7] containing the phenyl moiety is faster than the dissociation of the guest. Once guest dissociation becomes faster than Na^+ association, the complex is not stabilized, as observed at low Na^+ ion concentrations, and the complex is only transiently formed.

The switch in mechanism is only possible because of the opposing effects of Na^+ cations on the competitive formation of the two 1:1 complexes. In the absence of one of the two processes, no switch in mechanism would have been observed. In addition, knowledge of the individual equilibrium constants for the phenyl moiety binding to free CB[7] and Na^+ binding to free CB[7] is not sufficient to predict the synergistic formation of the capped complex Na^+•CB[7]@Ph-AH^+-Np, which then leads to the formation of the higher order 2:1 complex. Therefore, the active role of Na^+ in this host–guest system leads to the emergence of a new property and can be seen as an example of the bottom-up approach for understanding the effects of complexity in systems chemistry, where complexity in this case is related to the number of binding motifs in the guest and the role of the Na^+ cation.

The bottom-up approach is one of the angles from which systems chemistry can be studied. This approach relies on purposefully increasing the complexity of the system at the experimental design stage to determine the effect of this increased complexity on the system's behavior. We increased the complexity by using a ditopic guest with binding motifs of different sizes, so as to favor one complex thermodynamically. The intent was to explore how the transient binding of the smaller moiety affected the kinetics for the formation of the thermodynamic product. Na^+ ions were added to slow the kinetics to the millisecond time domain for the stopped-flow experiments, which is a strategy we have previously employed to study the CB[7] binding dynamics of a guest with one binding motif.[43] Our design for the ditopic guest worked at low Na^+ ion concentrations. However, the synergistic binding of the smaller binding motif of the guest and Na^+ with CB[7] combined with the opposing effects of Na^+ on the dissociation of the two 1:1 complexes increased the complexity of the system

beyond the original design. In addition to the intended thermodynamic complex, an additional complex formed in the same CB[7] concentration range, and the CB[7] complexation mechanism could be switched by changing the concentration ratios of the system's components. This study shows the value of the bottom-up approach to systems chemistry using kinetic studies, where the complexity of the system can be understood by observing the time evolution of the system toward equilibrium.

EXPERIMENTAL SECTION

Materials. Ph-A-Np (Aldrich, 97%) was recrystallized once from ethanol. Methanol (Fisher Chemicals, spectral grade, ≥99.9%), sodium chloride (Sigma-Aldrich, BioXtra, ≥99.5%), bis(cyclopentadienyl)cobalt(III) hexafluorophosphate (Cob^+, Aldrich, 98%), and a standardized volumetric solution of hydrochloric acid (4.0 N, Anachemia) were used as received. CB[7] was synthesized using a modified procedure based on previous literature[66–68] and purified as described elsewhere.[45] Deionized water (Barnstead NANOpure, ≥17.8 MΩ cm) was used to prepare all aqueous solutions.

Sample Preparation. A 700 μM stock solution of Ph-A-Np was prepared in methanol. Appropriate amounts of NaCl were dissolved in water containing HCl to prepare aqueous solutions with the required pH and NaCl concentrations. Stock solutions of CB[7] (≈1 mM) were prepared by dissolving the solid in aqueous solutions with the required NaCl concentration and pH. The CB[7] stock solutions were titrated with a Cob^+ solution to determine the actual CB[7] concentration.[69] Absorption measurements indicated that Ph-A-Np undergoes aggregation at concentrations of 5 μM or higher in water. The concentration of Ph-A-Np was therefore kept at 0.5 μM for all the measurements to prevent aggregation. For the steady-state and lifetime fluorescence experiments, 3 mL of the aqueous NaCl solution at pH 1.8 was placed in a cell and an appropriate volume of the Ph-A-Np stock solution was injected into the solution in the cell. Small volumes of the CB[7] stock solution were then injected into the cell. For stopped-flow experiments, several solutions with different CB[7] concentrations were prepared by diluting the stock solution in aqueous NaCl solutions at pH 1.8. The control solutions contained all chemicals except the fluorophore.

Equipment. Absorption measurements were performed with a Cary 100 spectrophotometer. Steady-state fluorescence measurements were performed with a PTI QM40 fluorimeter at 20 °C. Samples were excited at 303 nm and the emission was collected between 360 and 560 nm. The excitation and emission monochromator bandwidths were 2 nm. The emission spectrum of a control solution was subtracted from the spectrum of each sample.

Kinetic studies were performed on an Applied Photophysics SX20 stopped-flow system. The samples were excited at 303 nm using a Hg–Xe vapor lamp. The excitation monochromator bandwidth was set to 2.3 nm and the emission was collected using a cut-off filter that transmits light above 395 nm. The sample solutions were maintained at 20 °C for 5 min before an experiment was performed. The solutions were mixed in a 1:1 volume ratio in the mixing chamber. At least 20 kinetic traces were averaged to obtain a good signal-to-noise ratio. The averaged kinetic traces were corrected by subtracting the intensity of a solution containing all the components except Ph-A-Np. The analysis of the kinetic data and the fitting procedures are described in the Supporting Information.

Time-resolved fluorescence lifetime measurements were recorded on an Edinburgh Instruments OB920 single photon counting system. The samples were excited using a 310 nm light-emitting diode. The emission was collected at 438 nm using a monochromator with a 16 nm bandwidth. The number of counts in the maximum intensity channel was 2000. The instrument response function (IRF) was recorded with a light scattering solution of Ludox by recording the emission at the excitation wavelength. The analysis of the fluorescence decays and the fitting procedures are described in the Supporting Information.

ASSOCIATED CONTENT

Supporting Information

Estimation of pK_a values, quenching rate constant for excited Ph-AH-Np by acid, time-resolved fluorescence data, fitting model and binding isotherms, comparison of final intensities from binding isotherm and kinetic studies, kinetic data at low Na^+ concentrations, fluorescence data at high Na^+ concentrations, stopped-flow data at high Na^+ concentrations. The Supporting Information is available free of charge on the ACS Publications website as a PDF file.

AUTHOR INFORMATION

Corresponding Author

*cornelia.bohne@gmail.com

Present Addresses

† Current position: School of Chemistry and Chemical Engineering, South China University of Technology, 381 Wushan Road, Guangzhou 510641, China

Notes

The authors declare no competing financial interest.

ACKNOWLEDGMENT

The authors thank the Natural Sciences and Engineering Research Council of Canada (NSERC) for financial support (RGPIN-121389-2012, RGPIN-2017-04458).

REFERENCES

(1) Ashkenasy, G.; Hermans, T. M.; Otto, S.; Taylor, A. F. Systems Chemistry. *Chem. Soc. Rev.* **2017,** *46*, 2543–2554.

(2) Mattia, E.; Otto, S. Supramolecular Systems Chemistry. *Nat. Nanotechnol.* **2015,** *10*, 111–119.

(3) Giuseppone, N. Toward Self-Constructing Materials: A Systems Chemistry Approach. *Acc. Chem. Res.* **2012,** *45*, 2178–2188.

(4) Peyralans, J. J. P.; Otto, S. Recent Highlights in Systems Chemistry. *Curr. Opin. Chem. Biol.* **2009,** *13*, 705–713.

(5) Ludlow, R. F.; Otto, S. Systems Chemistry. *Chem. Soc. Rev.* **2008,** *37*, 101–108.

(6) Barrow, S. J.; Kasera, S.; Rowland, M. J.; del Barrio, J.; Scherman, O. A. Cucurbituril-Based Molecular Recognition. *Chem. Rev.* **2015,** *115*, 12320–12406.

(7) Cao, L.; Šekutor, M.; Zavalij, P. Y.; Mlinarić-Majerski, K.; Glaser, R.; Isaacs, L. Cucurbit[7]uril·Guest Pair with an Attomolar Dissociation Constant. *Angew. Chem., Int. Ed.* **2014,** *53*, 988–993.

(8) Dsouza, R. N.; Pischel, U.; Nau, W. M. Fluorescent Dyes and Their Supramolecular Host/Guest Complexes with Macrocycles in Aqueous Solution. *Chem. Rev.* **2011,** *111*, 7941–7980.

(9) Rekharsky, M. V.; Mori, T.; Yang, C.; Ko, Y. H.; Selvapalam, N.; Kim, H.; Sobransingh, D.; Kaifer, A. E.; Liu, S.; Isaacs, L.; Chen, W.; Moghaddam, S.; Gilson, M. K.; Kim, K.; Inoue, Y. A Synthetic Host-Guest System Achieves Avidin-Biotin Affinity by Overcoming Enthalpy–Entropy Compensation. *Proc. Natl. Acad. Sci. U. S. A.* **2007,** *104*, 20737–20742.

(10) Chernikova, E. Y.; Berdnikova, D. V.; Fedorov, Y. V.; Fedorova, O. A.; Maurel, F.; Jonusauskas, G. Light-Induced Piston Nanoengines: Ultrafast Shuttling of a Styryl Dye Inside Cucurbit[7]uril. *Phys. Chem. Chem. Phys.* **2017,** *19*, 25834–25839.

(11) Gürbüz, S.; Idris, M.; Tuncel, D. Cucurbituril-Based Supramolecular Engineered Nanostructured Materials. *Org. Biomol. Chem.* **2015,** *13*, 330–347.

(12) Assaf, K. I.; Nau, W. M. Cucurbiturils: From Synthesis to High-Affinity Binding and Catalysis. *Chem. Soc. Rev.* **2015,** *44*, 394–418.

(13) Mock, W. L.; Irra, T. A.; Wepsiec, J. P.; Adhya, M. Catalysis by Cucurbituril. The Significance of Bound-Substrate Destabilization for Induced Triazole Formation. *J. Org. Chem.* **1989,** *54*, 5302–5308.

(14) Palma, A.; Artelsmair, M.; Wu, G.; Lu, X.; Barrow, S. J.; Uddin, N.; Rosta, E.; Masson, E.; Scherman, O. A. Cucurbit[7]uril as a Supramolecular Artificial Enzyme for Diels–Alder Reactions. *Angew. Chem., Int. Ed.* **2017,** *56*, 15688–15692.

(15) Groombridge, A. S.; Palma, A.; Parker, R. M.; Abell, C.; Scherman, O. A. Aqueous Interfacial Gels Assembled from Small Molecule Supramolecular Polymers. *Chem. Sci.* **2017,** *8*, 1350–1355.

(16) Hwang, I.; Jeon, W. S.; Kim, H.-J.; Kim, D.; Kim, H.; Selvapalam, N.; Fujita, N.; Shinkai, S.; Kim, K. Cucurbit[7]uril: A Simple Macrocyclic, pH-Triggered Hydrogelator Exhibiting Guest-Induced Stimuli-Responsive Behavior. *Angew. Chem., Int. Ed.* **2007,** *46*, 210–213.

(17) Song, Q.; Gao, Y.; Xu, J.-F.; Qin, B.; Serpe, M. J.; Zhang, X. Supramolecular Microgels Fabricated from Supramonomers. *ACS Macro Lett.* **2016,** *5*, 1084–1088.

(18) Tan, C. S. Y.; del Barrio, J.; Liu, J.; Scherman, O. A. Supramolecular Polymer Networks Based on Cucurbit[8]uril Host–Guest Interactions as Aqueous Photo-Rheological Fluids. *Polym. Chem.* **2015,** *6*, 7652–7657.

(19) Dsouza, R. N.; Hennig, A.; Nau, W. M. Supramolecular Tandem Enzyme Assays. *Chem. - Eur. J.* **2012,** *18*, 3444–3459.

(20) Ghale, G.; Nau, W. M. Dynamically Analyte-Responsive Macrocyclic Host−Fluorophore Systems. *Acc. Chem. Res.* **2014,** *47*, 2150–2159.

(21) Hennig, A.; Bakirci, H.; Nau, W. M. Label-Free Continuous Enzyme Assays with Macrocycle-Fluorescent Dye Complexes. *Nat. Methods* **2007,** *4*, 629–632.

(22) Ghosh, I.; Nau, W. M. The Strategic Use of Supramolecular pK_a Shifts to Enhance the Bioavailability of Drugs. *Adv. Drug Delivery Rev.* **2012,** *64*, 764–783.

(23) Li, Q.-L.; Sun, Y.; Sun, Y.-L.; Wen, J.; Zhou, Y.; Bing, Q.-M.; Isaacs, L. D.; Jin, Y.; Gao, H.; Yang, Y.-W. Mesoporous Silica Nanoparticles Coated by Layer-by-Layer Self-Assembly Using Cucurbit[7]uril for in Vitro and in Vivo Anticancer Drug Release. *Chem. Mater.* **2014,** *26*, 6418–6431.

(24) Robinson-Duggon, J.; Pérez-Mora, F.; Dibona-Villanueva, L.; Fuentealba, D. Potential Applications of Cucurbit[*n*]urils Inclusion Complexes in Photodynamic Therapy. *Isr. J. Chem.* **2018,** *58*, 199–214.

(25) Samanta, S. K.; Moncelet, D.; Briken, V.; Isaacs, L. Metal–Organic Polyhedron Capped with Cucurbit[8]uril Delivers Doxorubicin to Cancer Cells. *J. Am. Chem. Soc.* **2016,** *138*, 14488–14496.

(26) Cera, L.; Schalley, C. A. Stimuli-Induced Folding Cascade of a Linear Oligomeric Guest Chain Programmed through Cucurbit[*n*]uril Self-Sorting (*n* = 6, 7, 8). *Chem. Sci.* **2014,** *5*, 2560–2567.

(27) Kotturi, K.; Masson, E. Directional Self-Sorting with Cucurbit[8]uril Controlled by Allosteric π–π and Metal–Metal Interactions. *Chem. - Eur. J.* **2018,** *24*, 8670–8678.

(28) Liu, S.; Ruspic, C.; Mukhopadhyay, P.; Chakrabarti, S.; Zavalij, P. Y.; Isaacs, L. The Cucurbit[*n*]uril Family: Prime Components for Self-Sorting Systems. *J. Am. Chem. Soc.* **2005,** *127*, 15959–15967.

(29) Mukhopadhyay, P.; Zavalij, P. Y.; Isaacs, L. High Fidelity Kinetic Self-Sorting in Multi-Component Systems Based on Guests with Multiple Binding Epitopes. *J. Am. Chem. Soc.* **2006,** *128*, 14093–14102.

(30) Buschmann, H.-J.; Cleve, E.; Jansen, K.; Wego, A.; Schollmeyer, E. Complex Formation between Cucurbit[n]urils and Alkali, Alkaline Earth and Ammonium Ions in Aqueous Solution. *J. Inclusion Phenom. Macrocyclic Chem.* **2001,** *40*, 117–120.

(31) Buschmann, H.-J.; Cleve, E.; Schollmeyer, E. Cucurbituril as a Ligand for the Complexation of Cations in Aqueous Solutions. *Inorg. Chim. Acta* **1992,** *193*, 93–97.

(32) Hoffmann, R.; Knoche, W.; Fenn, C.; Buschmann, H.-J. Host–Guest Complexes of Cucurbituril with the 4-Methylbenzylammonium Ion, Alkali-Metal Cations and NH_4^+. *J. Chem. Soc., Faraday Trans.* **1994,** *90*, 1507–1511.

(33) Masson, E.; Raeisi, M.; Kotturi, K. Kinetics Inside, Outside and Through Cucurbiturils. *Isr. J. Chem.* **2018,** *58*, 413–434.

(34) Neira, I.; García, M. D.; Peinador, C.; Kaifer, A. E. Terminal Carboxylate Effects on the Thermodynamics and Kinetics of Cucurbit[7]uril Binding to Guests Containing a Central Bis(Pyridinium)-Xylylene Site. *J. Org. Chem.* **2019,** *84*, 2325–2329.

(35) Mock, W. L.; Shih, N.-Y. Dynamics of Molecular Recognition Involving Cucurbituril. *J. Am. Chem. Soc.* **1989,** *111*, 2697–2699.

(36) Mock, W. L.; Shih, N.-Y. Structure and Selectivity in Host–Guest Complexes of Cucurbituril. *J. Org. Chem.* **1986,** *51*, 4440–4446.

(37) Miskolczy, Z.; Megyesi, M.; Toke, O.; Biczók, L. Change of the Kinetics of Inclusion in Cucurbit[7]uril upon Hydrogenation and Methylation of Palmatine. *Phys. Chem. Chem. Phys.* **2019,** *21*, 4912–4919.

(38) Miskolczy, Z.; Biczók, L.; Jablonkai, I. Kinetics of the Reversible Inclusion of Flavopereirine in Cucurbit[7]uril. *Phys. Chem. Chem. Phys.* **2017,** *19*, 766–773.

(39) Marquez, C.; Nau, W. M. Two Mechanisms of Slow Host–Guest Complexation between Cucurbit[6]uril and Cyclohexylmethylamine: pH-Responsive Supramolecular Kinetics. *Angew. Chem., Int. Ed.* **2001,** *40*, 3155–3160.

(40) Márquez, C.; Hudgins, R. R.; Nau, W. M. Mechanism of Host−Guest Complexation by Cucurbituril. *J. Am. Chem. Soc.* **2004,** *126*, 5806–5816.

(41) Ling, Y.; Mague, J. T.; Kaifer, A. E. Inclusion Complexation of Diquat and Paraquat by the Hosts Cucurbit[7]uril and Cucurbit[8]uril. *Chem. - Eur. J.* **2007,** *13*, 7908–7914.

(42) Appel, E. A.; Biedermann, F.; Hoogland, D.; del Barrio, J.; Driscoll, M. D.; Hay, S.; Wales, D. J.; Scherman, O. A. Decoupled Associative and Dissociative Processes in Strong yet Highly Dynamic Host–Guest Complexes. *J. Am. Chem. Soc.* **2017,** *139*, 12985–12993.

(43) Tang, H.; Fuentealba, D.; Ko, Y. H.; Selvapalam, N.; Kim, K.; Bohne, C. Guest Binding Dynamics with Cucurbit[7]uril in the Presence of Cations. *J. Am. Chem. Soc.* **2011,** *133*, 20623–20633.

(44) Miskolczy, Z.; Biczók, L. Kinetics and Thermodynamics of Berberine Inclusion in Cucurbit[7]uril. *J. Phys. Chem. B* **2014,** *118*, 2499–2505.

(45) Thomas, S. S.; Bohne, C. Determination of the Kinetics Underlying the pK_a Shift for the 2-Aminoanthracenium Cation Binding with Cucurbit[7]uril. *Faraday Discuss.* **2015,** *185*, 381–398.

(46) Held, B.; Tang, H.; Natarajan, P.; da Silva, C. P.; de Oliveira Silva, V.; Bohne, C.; Quina, F. H. Cucurbit[7]uril Inclusion Complexation as a Supramolecular Strategy for Color Stabilization of Anthocyanin Model Compounds. *Photochem. Photobiol. Sci.* **2016,** *15*, 752–757.

(47) Megyesi, M.; Biczók, L.; Jablonkai, I. Highly Sensitive Fluorescence Response to Inclusion Complex Formation of Berberine Alkaloid with Cucurbit[7]uril. *J. Phys. Chem. C* **2008,** *112*, 3410–3416.

(48) Ong, W.; Kaifer, A. E. Salt Effects on the Apparent Stability of the Cucurbit[7]uril−Methyl Viologen Inclusion Complex. *J. Org. Chem.* **2004,** *69*, 1383–1385.

(49) Rekharsky, M. V.; Ko, Y. H.; Selvapalam, N.; Kim, K.; Inoue, Y. Complexation Thermodynamics of Cucurbit[6]uril with Aliphatic Alcohols, Amines, and Diamines. *Supramol. Chem.* **2007,** *19*, 39–46.

(50) Shaikh, M.; Mohanty, J.; Bhasikuttan, A. C.; Uzunova, V. D.; Nau, W. M.; Pal, H. Salt-Induced Guest Relocation from a Macrocyclic Cavity into a Biomolecular Pocket: Interplay between Cucurbit[7]uril and Albumin. *Chem. Commun.* **2008,** 3681–3683.

(51) Wyman, I. W.; Macartney, D. H. Cucurbit[7]uril Host–Guest Complexes with Small Polar Organic Guests in Aqueous Solution. *Org. Biomol. Chem.* **2008,** *6*, 1796–1801.

(52) Jeon, Y.-M.; Kim, J.; Whang, D.; Kim, K. Molecular Container Assembly Capable of Controlling Binding and Release of Its Guest Molecules: Reversible Encapsulation of Organic Molecules in Sodium Ion Complexed Cucurbituril. *J. Am. Chem. Soc.* **1996,** *118*, 9790–9791.

(53) El Haouaj, M.; Ko, Y. H.; Luhmer, M.; Kim, K.; Bartik, K. NMR Investigation of the Complexation of Neutral Guests by Cucurbituril. *J. Chem. Soc., Perkin Trans. 2* **2001**, 2104–2107.

(54) Whang, D.; Heo, J.; Park, J. H.; Kim, K. A Molecular Bowl with Metal Ion as Bottom: Reversible Inclusion of Organic Molecules in Cesium Ion Complexed Cucurbituril. *Angew. Chem., Int. Ed.* **1998,** *37*, 78–80.

(55) Shinde, M. N.; Dutta Choudhury, S.; Barooah, N.; Pal, H.; Bhasikuttan, A. C.; Mohanty, J. Metal-Ion-Mediated Assemblies of Thiazole Orange with Cucurbit[7]uril: A Photophysical Study. *J. Phys. Chem. B* **2015,** *119*, 3815–3823.

(56) Mock, W. L.; Pierpont, J. A Cucurbituril-Based Molecular Switch. *J. Chem. Soc., Chem. Commun.* **1990,** 1509–1511.

(57) Saleh, N.; Koner, A. L.; Nau, W. M. Activation and Stabilization of Drugs by Supramolecular pK_a Shifts: Drug-Delivery Applications Tailored for Cucurbiturils. *Angew. Chem., Int. Ed.* **2008,** *47*, 5398–5401.

(58) Barooah, N.; Mohanty, J.; Pal, H.; Bhasikuttan, A. C. Cucurbituril-Induced Supramolecular pK_a Shift in Fluorescent Dyes and Its Prospective Applications. *Proc. Natl. Acad. Sci., India, Sect. A* **2014,** *84*, 1–17.

(59) Li, S.; Yin, H.; Wyman, I. W.; Zhang, Q.; Macartney, D. H.; Wang, R. Encapsulation of Vitamin B_1 and Its Phosphate Derivatives by Cucurbit[7]uril: Tunability of the Binding Site and Affinity by the Presence of Phosphate Groups. *J. Org. Chem.* **2016,** *81*, 1300–1303.

(60) Pischel, U.; Uzunova, V. D.; Remón, P.; Nau, W. M. Supramolecular Logic with Macrocyclic Input and Competitive Reset. *Chem. Commun.* **2010,** *46*, 2635–2637.

(61) Förster, T. Deactivation by Proton Transfer in the Excited State. *Chem. Phys. Lett.* **1972,** *17*, 309–311.

(62) Tsutsumi, K.; Shizuka, H. Excited State pK^*_a Values of Naphthylamines: Proton-Induced Fluorescence Quenching. *Chem. Phys. Lett.* **1977,** *52*, 485–488.

(63) Wagner, B. D.; Stojanovic, N.; Day, A. I.; Blanch, R. J. Host Properties of Cucurbit[7]uril: Fluorescence Enhancement of Anilinonaphthalene Sulfonates. *J. Phys. Chem. B* **2003,** *107*, 10741–10746.

(64) Basílio, N.; Laia, C. A. T.; Pina, F. Excited-State Proton Transfer in Confined Medium. 4-Methyl-7-hydroxyflavylium and β-Naphthol Incorporated in Cucurbit[7]uril. *J. Phys. Chem. B* **2015,** *119*, 2749–2757.

(65) Da Silva, J. P.; Jayaraj, N.; Jockusch, S.; Turro, N. J.; Ramamurthy, V. Aggregates of Cucurbituril Complexes in the Gas Phase. *Org. Lett.* **2011,** *13*, 2410–2413.

(66) Day, A. I.; Blanch, R. J.; Arnold, A. P.; Lorenzo, S.; Lewis, G. R.; Dance, I. A Cucurbituril-Based Gyroscane: A New Supramolecular Form. *Angew. Chem., Int. Ed.* **2002,** *41*, 275–277.

(67) Kim, J.; Jung, I.-S.; Kim, S.-Y.; Lee, E.; Kang, J.-K.; Sakamoto, S.; Yamaguchi, K.; Kim, K. New Cucurbituril Homologues: Syntheses, Isolation, Characterization, and X-ray Crystal Structures of Cucurbit[*n*]uril (*n* = 5, 7, and 8). *J. Am. Chem. Soc.* **2000,** *122*, 540–541.

(68) Marquez, C.; Huang, F.; Nau, W. M. Cucurbiturils: Molecular Nanocapsules for Time-Resolved Fluorescence-Based Assays. *IEEE Trans. Nanobiosci.* **2004,** *3*, 39–45.

(69) Yi, S.; Kaifer, A. E. Determination of the Purity of Cucurbit[*n*]uril (*n* = 7, 8) Host Samples. *J. Org. Chem.* **2011,** *76*, 10275–10278.

TOC

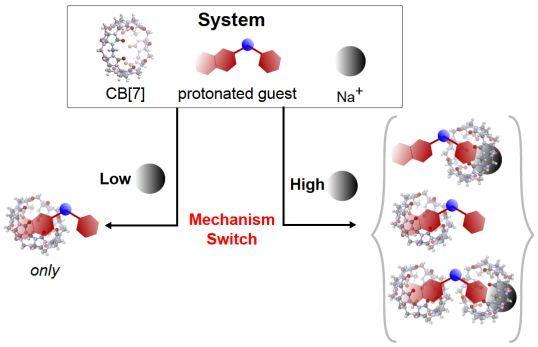
System
CB[7]
protonated guest
Na+
Low
High
Mechanism
Switch
only